

MICROCOPY RESOLUTION TEST CHART

NBS - 1010a

(ANSI and ISO TEST CHART No. 2)



4.5



5.0

5.6



6.3



7.1

8.0



9.0

10

11.2



PHOTOGRAPHIC SCIENCES CORPORATION

770 BASKET ROAD

P.O. BOX 338

WEBSTER, NEW YORK 14580

(716) 265-1600

95 00135

Dipartimento Innovazione

TRIPLE STATE OPTICAL INVESTIGATION OF THE F_3^+ COLOR CENTER IN LIF

G. BALDACCHINI, R.M. NONTERALI
Centro Ricerche di Frascati, Roma

M. CREMONA, G. D'AURIA
ENEA Guest

V. KALINOV
Institute of Molecular and Atomic Physics, Academy of Sciences of Belarus, Minsk, Belarus



ENTE PER LE NUOVE TECNOLOGIE,
L'ENERGIA E L'AMBIENTE

Dipartimento Innovazione

TRIPLE STATE OPTICAL INVESTIGATION OF THE F_3^+ COLOR CENTER IN LiF

G. BALDACCHINI, R.M. NONTERALI
Centro Ricerche di Frascati, Roma

M. CREMONA, G. D'AURIA
ENEA Guest

V. KALINOV
Institute of Molecular and Atomic Physics, Academy of Sciences of Belarus, Minsk, Belarus

RT/INN/94/52

VOL

Manuscript received in final form on November 1994

This report has been prepared, and distributed by: *Servizio Edizioni Scientifiche* - ENEA, Centro Ricerche Frascati, C.P. 65 - 00044 Frascati, Rome, Italy.

Published by ENEA, Direzione Relazioni Esterne, Viale Regina Margherita 125, Rome, Italy

SUMMARY

Several color centers, which are of some interest for pulsed laser emission, can be produced in LiF crystals. Among these centers, which are stable at room temperature under optical pumping, the F_3^+ center, after absorbing at ~ 450 nm, displays an emission at ~ 535 nm, which has unusual dependences on time, excitation power, and temperature. A triplet state in the optical cycle can explain its peculiar properties, and in this work an accurate study of the absorption and emission has been accomplished as a function of temperature. These measurements have shown the existence of multiphonon processes in the energy transfer transitions to and from the triplet state. Moreover better conditions for laser action have been found at temperatures lower than RT, where there is the possibility of having a c.w. laser emission.

RIASSUNTO

Nel LiF possono essere prodotti molti centri di colore che sono interessanti per la realizzazione di laser impulsati. Tra questi centri stabili a temperatura ambiente sotto pompaggio ottico, il centro F_3^+ , dopo essere stato eccitato a ~ 450 nm, emette a ~ 535 nm con peculiari caratteristiche temporali dipendenti dalla potenza di pompaggio e dalla temperatura. Uno stato di tripletto nel ciclo ottico può spiegare queste proprietà, ed in questo lavoro vengono studiate accuratamente l'assorbimento e l'emissione in funzione della temperatura. Le misure effettuate hanno mostrato l'esistenza di processi multifononici nelle transizioni per e dallo stato di tripletto. In più si è trovato che a temperature inferiori a quella ambiente, le condizioni per l'emissione laser sono migliori, facendo intravedere la possibilità di ottenere un regime laser continuo.

INDEX

1	INTRODUCTION	p. 7
2	FOTOCHEMISTRY OF F_2 AND F_3^+ COLOR CENTERS	p. 8
3	EXPERIMENTAL	p. 11
4	DISCUSSION	p. 19
5	CONCLUSIONS	p. 27
	ACKNOWLEDGEMENTS	p. 28
	REFERENCES	p. 29

TRIPLET STATE OPTICAL INVESTIGATION OF THE F_3^+ COLOR CENTER IN LiF

1 - INTRODUCTION

The search for laser radiation tunable in a wide spectral range has been under way since the sixties in solid-state active media. Among them alkali halide crystals with intrinsic color centers have shown to be suitable materials [1]. In particular lithium fluoride is one of the most popular among them both for its good physical properties and for the thermal stability of its color centers, which can be manipulated at room temperature [2,3]. In its original state the LiF crystal is colorless. Under the action of γ -rays, high-energy electrons and X-rays, intrinsic point defects appear in this crystal, giving rise to characteristic colorings. In LiF, and in the other alkali halides, the defect with the simplest structure is the F center, an anion vacancy which has captured one electron. All color centers which have lased up to now are complexes derived from F centers. For instance, the F_2 center consists of two neighbour vacancies with two captured electrons, and the F_3^+ center is composed of three vacancies with two captured electrons.

The emission of the color centers which are used for laser action takes place according to a well known 4-level scheme. Pump radiation is absorbed in a broad vibronic band, which subsequently relaxes via nonradiative processes to the minimum of the nuclear or lattice potential curve of the excited state in a time of 10^{-12} - 10^{-13} s. After that a radiative transition, which produces the characteristic luminescence, occurs with a time of 10^{-6} - 10^{-9} s toward the lower state, which quickly relaxes to the potential minimum of the ground state. Color center lasers in ionic crystals have become a new class of sources of coherent radiation, and they possess unique characteristics such as high frequency stability and an extremely narrow spectral width, achievable virtually without power losses, while maintaining a practically important wide spectral region of tuning from 0.5 to 4 μm , due to the homogeneous broadening of their optical gain transitions. Moreover the superb characteristics obtained by available and simple laser techniques, and the capability of color center lasers to operate efficiently in all known temporal modes, continuous to subpicosecond pulse, make them important tools for both basic and applied experimental physics.

Studies on LiF based lasers have established that lasing at room temperature and in pulsed regime is possible in the spectral ranges 0.65-0.74 μm (F_2 centers), 0.84-1.12 μm (F_2^+ centers), 1.09-1.26 μm (F_2^- centers), and 0.51 - 0.57 μm (F_3^+ centers) [3,4,5].

Besides their unique and advantageous properties, in several alkali halide crystals color centers have some shortcomings. For example, laser oscillation can be suppressed by competing processes such as optical bleaching and degradation under pump radiation, spontaneous thermal or thermo-optical degradation at room temperature, the presence of absorption bands in the emission region, absorption from the excited state, transitions to triplet states, overlapping of absorption bands from different centers, and radiationless transitions [3,4,6]. In LiF crystals the losses listed above can be either completely eliminated or usefully controlled, with the exception of those due to the triplet state, which up to now has not been widely investigated, while a better understanding of their basic mechanisms would be very important for fundamental research, and to contemplate continuous pumping experiments.

The present paper is devoted to an accurate study of the optical characteristics of F_2 and F_3^+ centers in LiF, which display unusual behaviours connected with the existence of a triplet state under irradiation by the 457 nm line of an argon laser [7,8].

2 - FOTOCHEMISTRY OF F_2 AND F_3^+ COLOR CENTERS

It is well known that excitation in the F_2 band (450 nm) of the LiF crystals produces a green emission peaked at about 535 nm and a red one at about 670 nm. Polarization measurements and optical investigations have shown that the defects responsible for the green and red emissions are the F_3^+ and F_2 centers respectively [9]. The F_3^+ absorption band has a maximum at 458 nm, and it almost coincides with the F_2 absorption band, whose maximum is at 441 nm. The overlapping of the two absorption bands allows the simultaneous lasing in the green and red spectral regions [7,10,11]. But such coincidence produces serious difficulties for the preparation of active media with low losses at the pumping wavelengths (400-490 nm) and for the laser oscillation of F_3^+ color centers (510-570 nm) alone. The F_2 color centers are not photostable, and under pumping they produce F_2^+ centers which, with their absorption band peaked at 645 nm, introduce losses to the F_2 laser emission. Moreover, by using the ordinary technology of coloring of LiF crystals by X-rays or electron beams at room temperature, the concentration of F_2 centers is higher than that of F_3^+ ones. For these reasons, and also because of the existence of N centers absorbing the F_3^+ luminescence at 540 nm, the efficiency of pumping the F_3^+ color centers is very low. In previous works these difficulties have been overcome by irradiating the samples at liquid nitrogen [7] and at dry ice temperatures [10,11]. The samples produced under these conditions have the following characteristics:

- a) the color of the crystals is green;
- b) the excitation at 450 nm gives a strong green emission band due to F_3^+ centers and a weak red one of F_2 centers (Fig. 1);
- c) there is no N center absorption.

The technology to create color centers in Ref.10 differs from that described in Ref. 7 for the use of γ -rays instead of electron beams, the former producing samples of large dimensions with a homogeneous distribution of color centers. With such γ -irradiated samples, simultaneous emission in the regions from 520 to 560 nm and from 640 to 680 nm, due to F_3^+ and F_2 color centers respectively, is observed under intense pumping [11], but the emission of F_2 color centers decreases after a few tens of pulses by more than two orders of magnitude. Within the experimental errors the emission in the green spectral region remains practically unchanged. So, in order to increase this green luminescence it is necessary, at the stage of preparation of the active medium, to eliminate the F_2 color centers. For this purpose the pumping of an excimer laser at the wavelength of 308 nm was used [11], being this wavelength within the second absorption band of F_2 color centers [12,13]. Excimer laser radiation destroys effectively F_2 color centers, which are converted into F_3^+ centers. Indeed during such light treatment the concentration of F_3^+ color centers increases.

Figure 2 shows the absorption (a) and luminescence (b) spectra of a lithium fluoride crystal with F_3^+ and F_2 color centers before the treatment with the excimer laser radiation (curves 1,4), immediately after pumping with 100 pulses characterized by an average power density of about 10 MW/cm² (curve 2), and one day after such treatment, (curves 3,5). The decreasing of the absorption band at 450 nm immediately

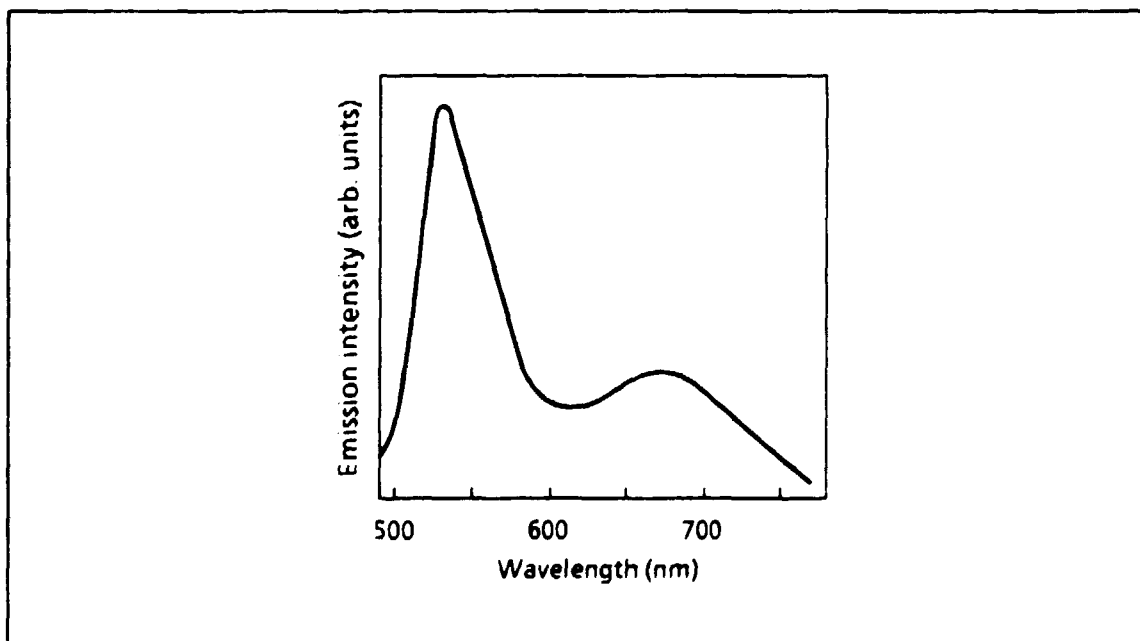


Fig. 1 - RT emission spectrum due to excitation at 450 nm of a LiF crystal γ -irradiated at dry ice temperature

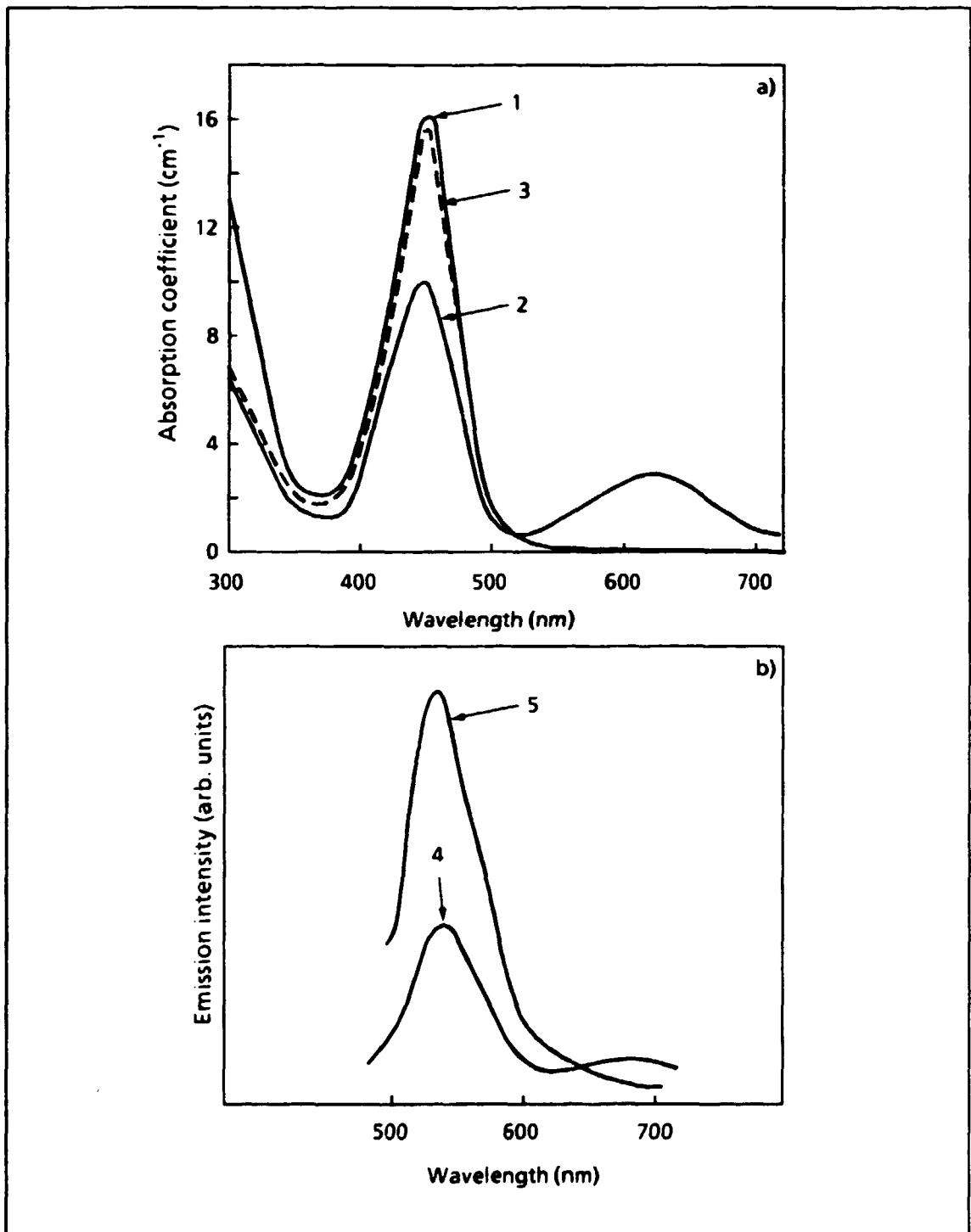


Fig. 2 - RT absorption, a, and luminescence spectra excited at 450 nm, b, of a γ -irradiated LiF crystal before excimer laser irradiation (1,4), just after irradiation (2), and 24 hours later (3,5)

after pumping is due to the conversion of F_2 to F_2^+ color centers, which have the absorption band peaked at 645 nm. Afterward there is a further conversion of F_2^+ to F_3^+ defects, as indicated by absorption and luminescence spectra before and after such treatment.

So with this procedure it is possible to remove almost completely the F_2 centers and to increase the concentration of F_3^+ centers. It is evident from the luminescence spectra (Fig. 2b) that one pumping annealing cycle at room temperature can reduce the intensity of the luminescence of the F_2 centers to a negligible value compared to the intensity of the F_3^+ centers. F_3^+ color centers, generated with the previous recipe, exhibit high thermostability and photostability to blue pump radiation. Even during laser operation no bleaching effects and decline of laser output power of F_3^+ color centers was observed [11]. The active medium LiF:F_3^+ is stable at room temperature and can withstand brief heatings to fairly high temperatures without any measurable fading effects.

3 - EXPERIMENTAL

F_2 , F_3^+ and other color centers (mainly F and F_3) were produced at a temperature of -60°C (dry ice temperature) by γ -rays from a ^{60}Co source. The exposure rate at the sample position was $0.7\text{ kC}/(\text{kg}\cdot\text{h})$ (equivalent to $2.79 \cdot 10^6\text{ R/h}$) and the dose of irradiation was 7 kC/kg . The sample used in the experiments, of dimensions $20 \times 40 \times 1.15\text{ mm}^3$, was placed in a cryostat with temperature variable from RT to LNT. The absorption and emission measurements were taken with the experimental apparatus reported in Fig. 3. Emission measurements were taken both in a colinear

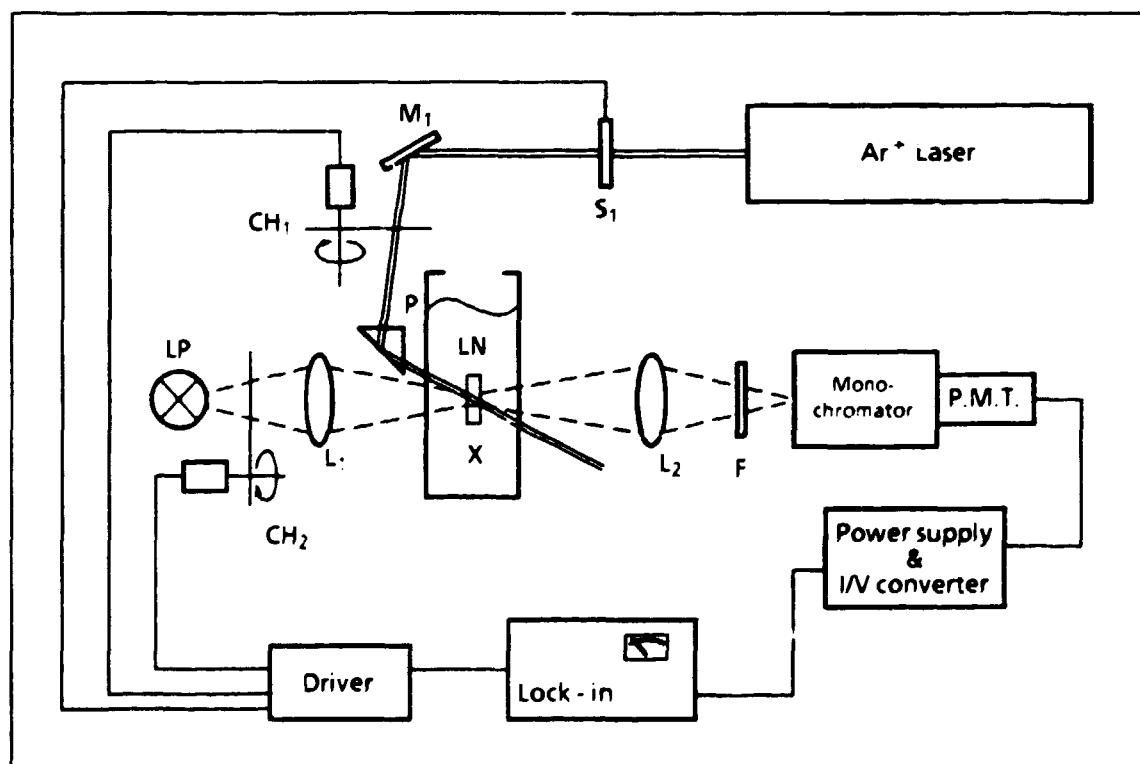


Fig. 3 - Experimental set-up used for the emission and absorption measurements

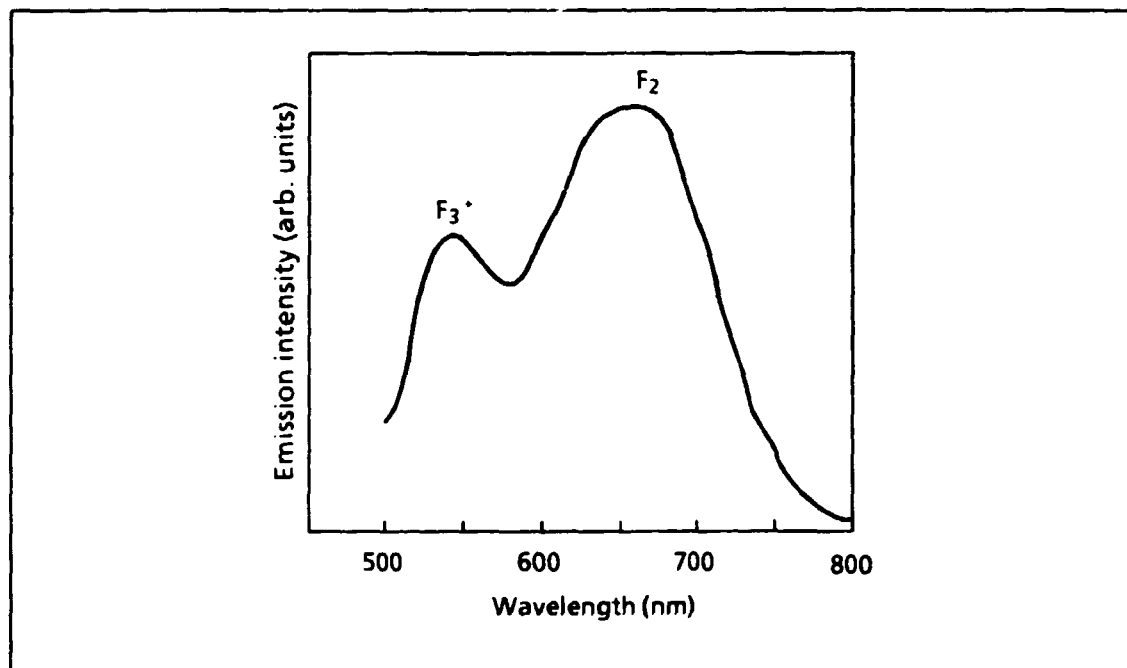


Fig. 4 - Emission spectrum of the LiF crystal under pumping with the 457 nm line of an Argon laser

and perpendicular geometry of the pumping source and detector. The 457 nm line of an argon ion laser was used to excite both F_2 and F_3^+ color centers, which have almost coincident absorption bands centered around 450 nm. A photomultiplier with S20 response was used for monitoring the emission collected through a 10 cm focal length monochromator. The pumping light was modulated by a chopper and the signal analyzed by the lock-in technique. Before and after each emission measurement, absorption spectra were recorded, by using a Perkin Elmer 330 spectrophotometer, in order to check whether some changes had occurred in the sample during the luminescence experiments. The absorption at the fixed wavelength of 460 nm under 457 nm laser pumping was monitored by using the light from a tungsten lamp, and the signal from the photomultiplier was sent to a logarithmic amplifier.

Figure 4 shows the luminescence spectrum of the sample at RT after the sole γ -rays irradiation under the argon laser pumping. As expected, the sample contains more F_2 than F_3^+ centers. However a treatment as described in the previous section gets rid almost entirely of the presence of F_2 centers, as demonstrated by the emission spectrum of Fig. 5, which shows only a small residual F_2 luminescence, and by the absorption spectrum of Fig. 6, which practically shows only F and among F aggregated centers mainly F_3^+ centers (the presence of F_3^+ centers is revealed by the width of their absorption band which is slightly larger with respect to that when mainly F_2 centers are also present). During the emission measurements reported in Fig. 4, a significant change of color of the crystal from green to yellow has been observed in the first seconds of laser pumping. A similar but much less marked coloring change has also been observed in the crystal after photochemical treatment, whose emission is reported in Fig. 5. However in this case a decrease of the emission intensity was observed at naked eyes.

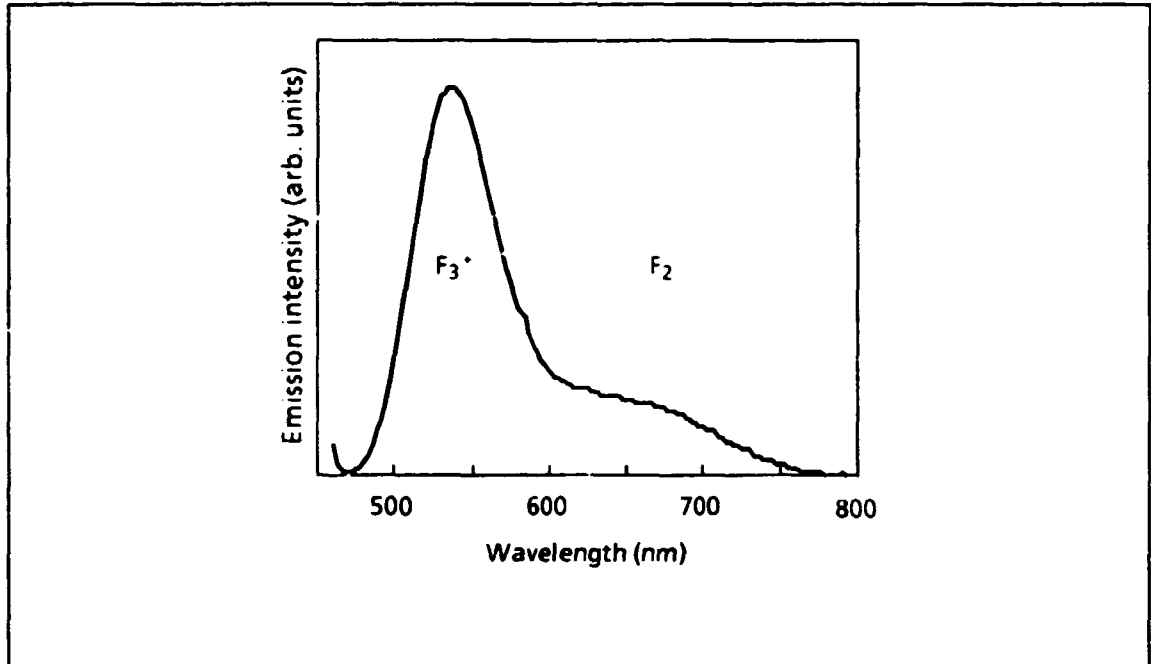


Fig. 5 - Emission spectrum of the crystal as in Fig. 4 after photochemical treatment as in the text under the same pumping conditions

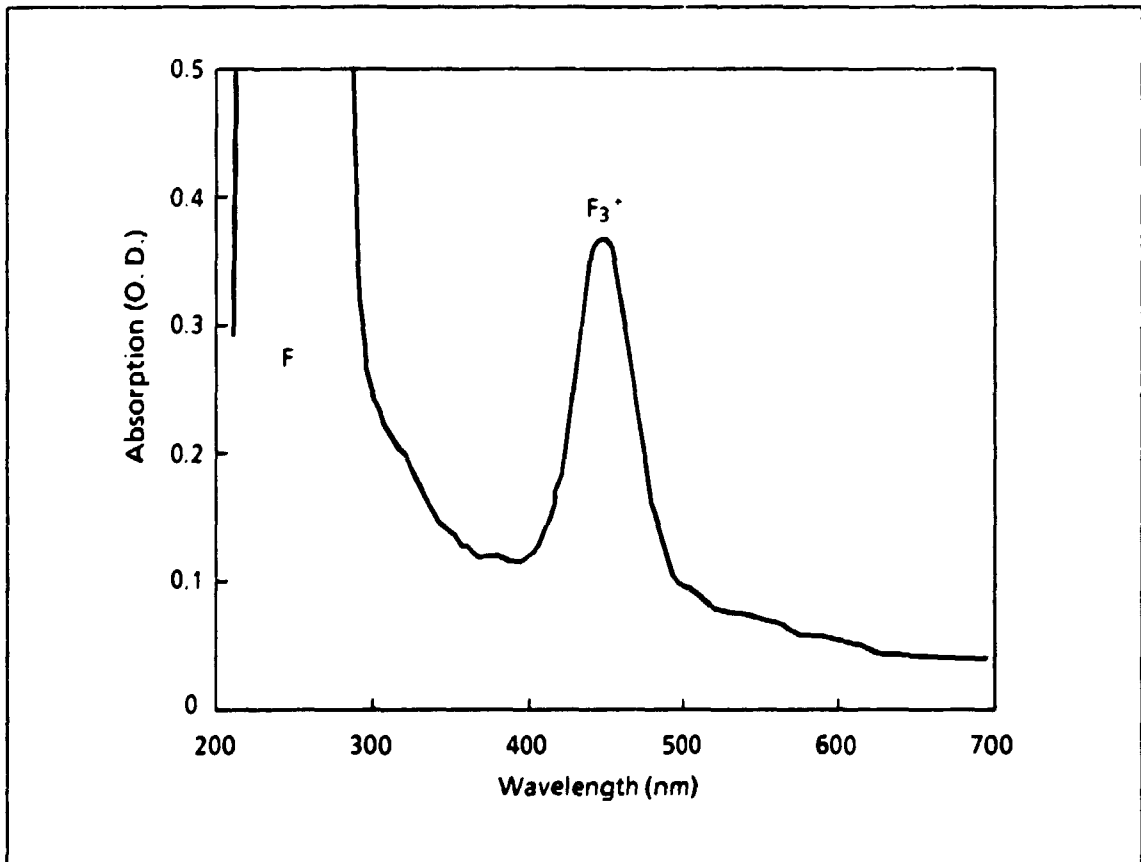


Fig. 6 - Absorption spectrum at RT of the LiF crystal as in Fig. 5 (1.15 mm thick, irradiated with γ rays at -60°C)

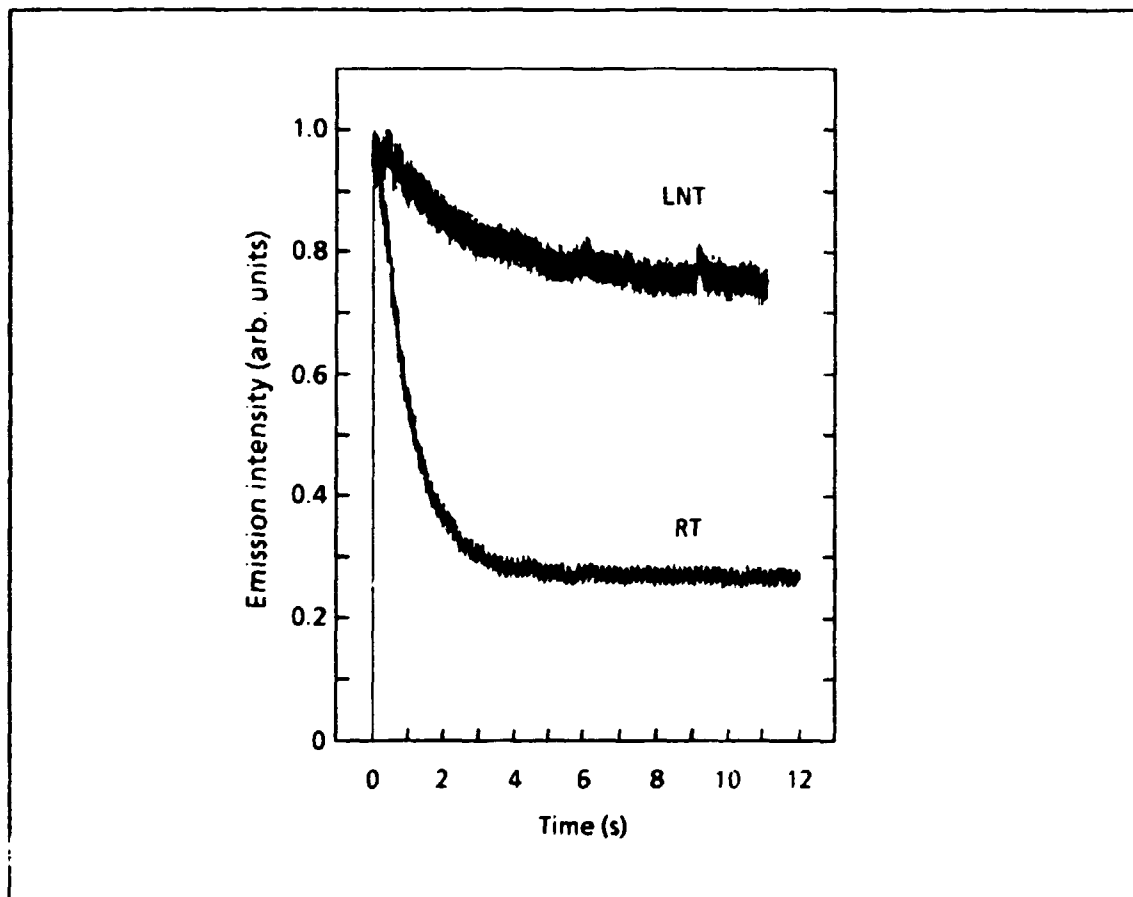


Fig. 7 - Time evolution of the emission at 520 nm after switching on the laser excitation at 457 nm at a power of 42.5 mW at RT and LNT

These anomalous properties prompted us to make accurate measurements of the temporal evolution of the emission after the onset of laser pumping. Figure 7 shows the emission intensity at 520 nm after switching on with a scanner the pumping laser excitation. An analogous experiment performed with another sample containing only F_2 centers did not show any intensity variation of the emission at ~ 670 nm. The sample with F_2 centers alone was obtained by heating at ~ 200 °C for 2 hours a crystal containing both F_3^+ and F_2 centers.

The previous experiments demonstrate that the time evolution of the emission intensity is due only to the F_3^+ centers. The change of color in the sample of Fig. 4 is due to the decrease of the green F_3^+ luminescence, while the red F_2 luminescence remains constant at the used power levels. The temporal evolution is spectrally homogeneous on the whole F_3^+ emission band, as shown in Figs. 8a and 8b, where the initial and final values of the emission intensity are reported for RT and LNT measurements respectively.

The emission intensity at 520 nm as a function of the pumping power is reported in Figs. 9a and 9b for RT and LNT respectively. They show unambiguously that the initial

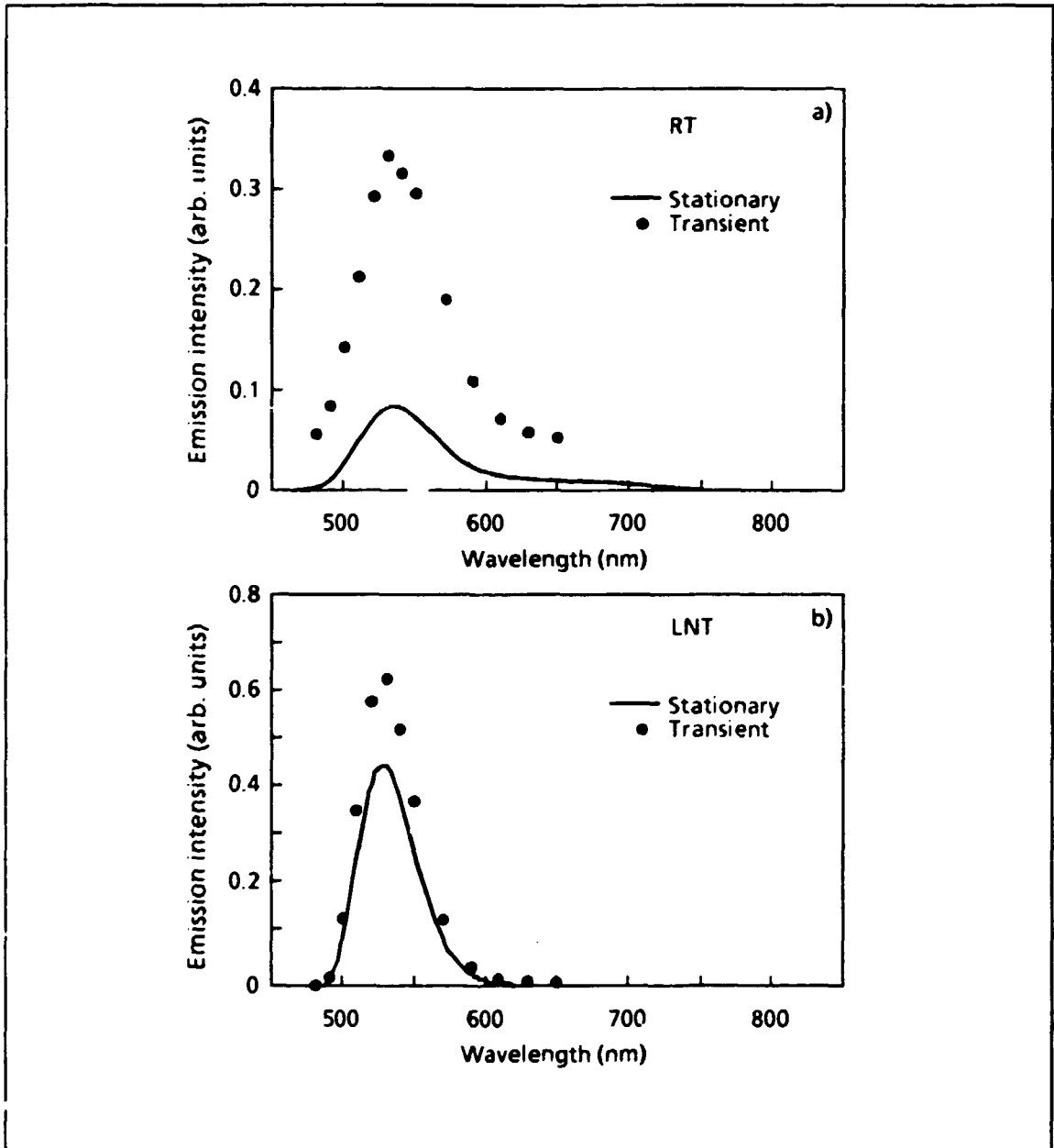


Fig. 8 - Initial (transient) and final (stationary) F_3^+ emission band under laser irradiation with the 457 nm line of an Ar laser with a power of 42.5 mW at RT, a, and LNT, b

value of the emission is linear with the power, while the final one displays a saturation effect.

Similar behaviours have also been observed in the absorption spectrum of the F_3^+ center. Figure 10 shows the time evolution of the absorption at 450 nm after switching on and off the pump laser.

The time behaviour of the signal variations in Figs. 7 and 10 can be described by exponential curves with a unique time constant τ_p (pumping) when the laser is

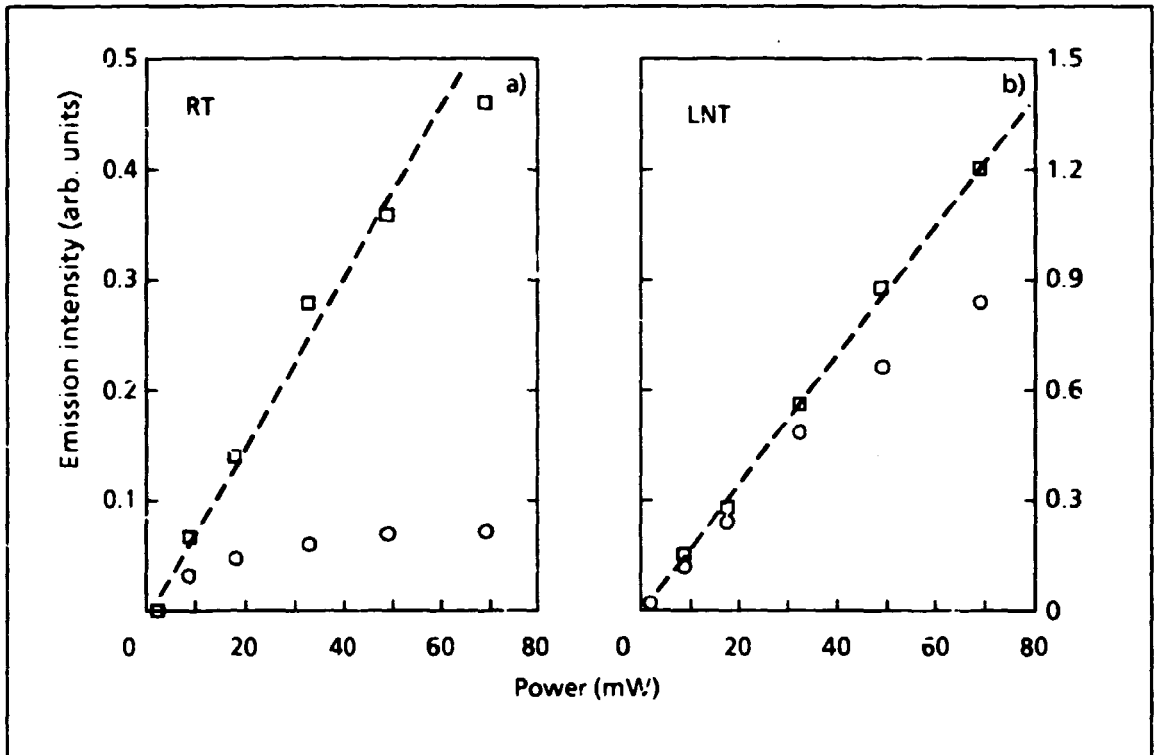


Fig. 9 - Initial (squares) and final (circles) values of the emission intensity at 520 nm as a function of the pumping power of the 457 nm line of an Ar laser at RT, a, and LNT, b

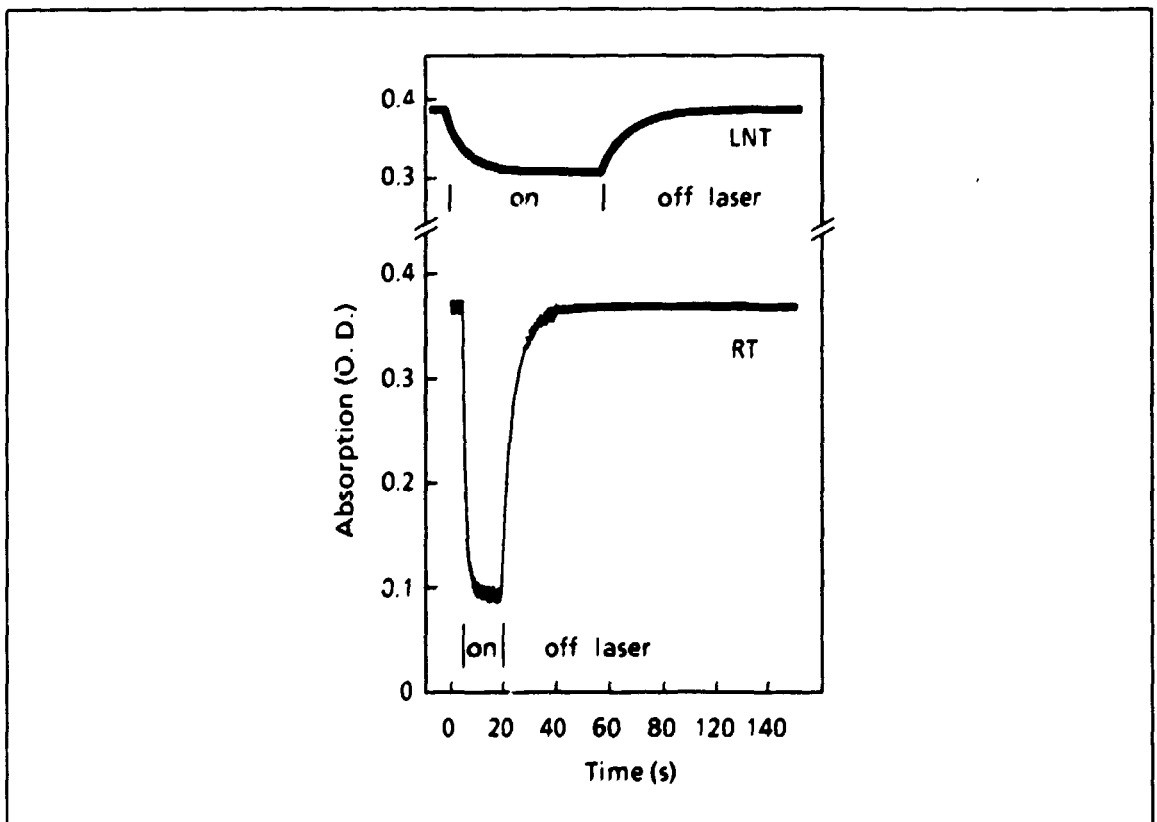


Fig. 10 - Time evolution of the F_3^+ absorption at 450 nm after switching on and off the laser excitation at 457 nm with a power of 42.5 mW at RT and LNT

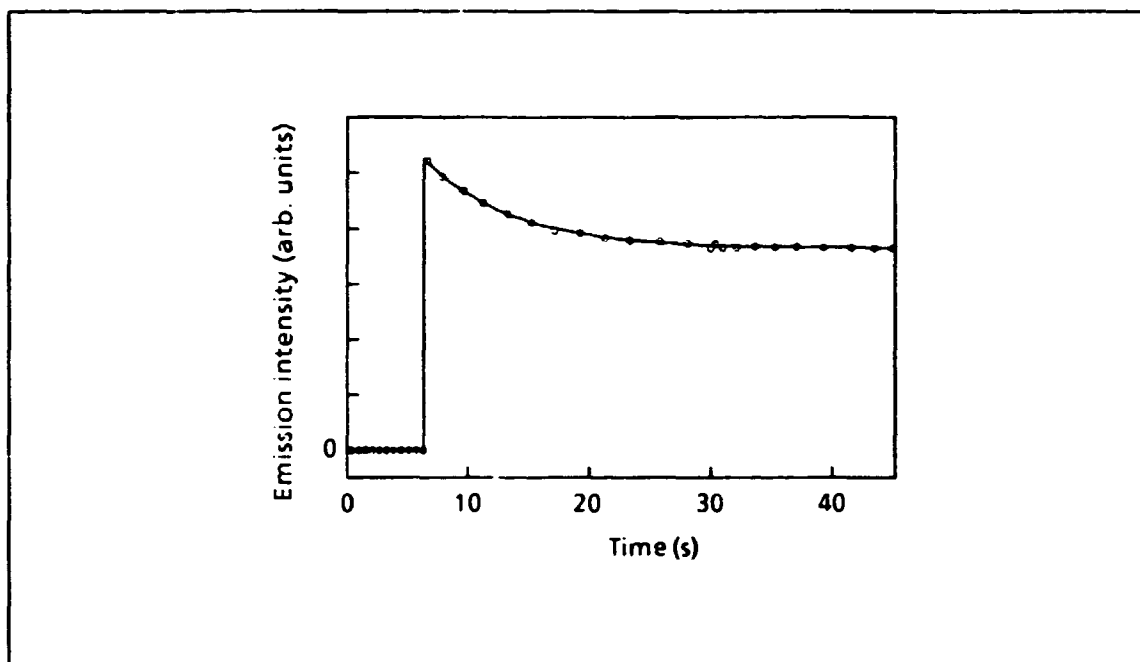


Fig. 11 - Time dependence of the luminescence at LNT after switching on the laser pumping (circles), and fitting with an exponential curve with a unique time constant $\tau_p = 7.20$ s (continuous line)

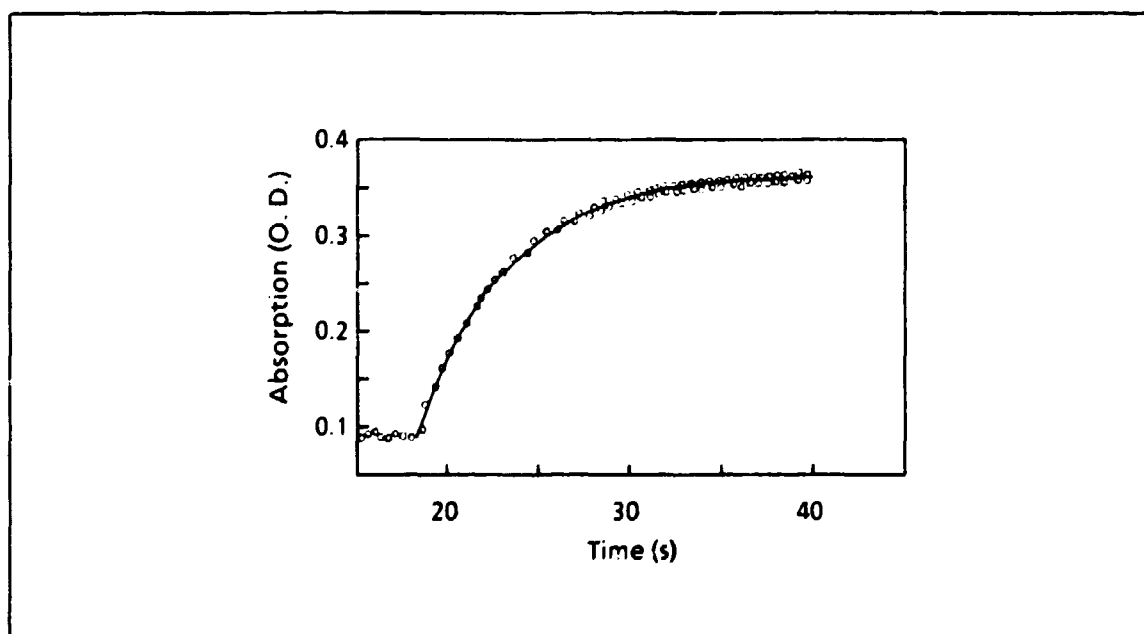


Fig. 12 - Time dependence of the absorption at RT after switching off the laser pumping (circles), and fitting with an exponential curve with a unique time constant $\tau_r = 4.86$ s (continuous line)

switched on, and τ_r (recovery) when the laser is switched off. Figures 11 and 12 show two typical fittings of experimental results at LNT and RT respectively, and the agreement is very good. The time constant τ_p has been measured as a function of

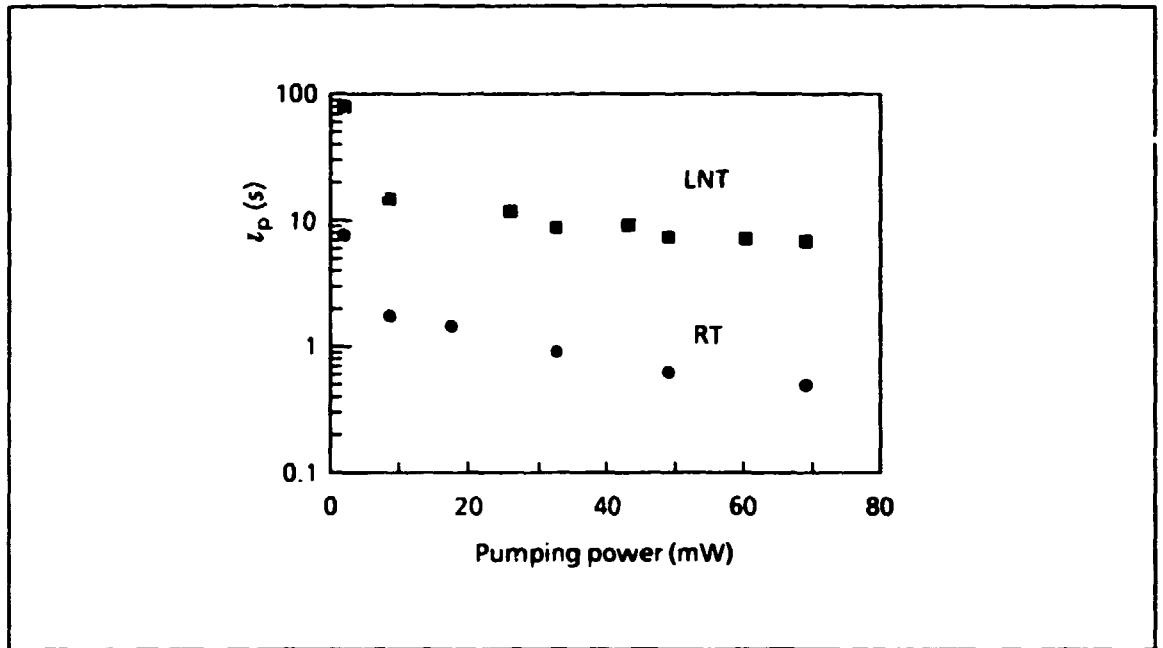


Fig. 13 - Time constant τ_p as a function of pumping power at RT and LNT, obtained from the emission measurements

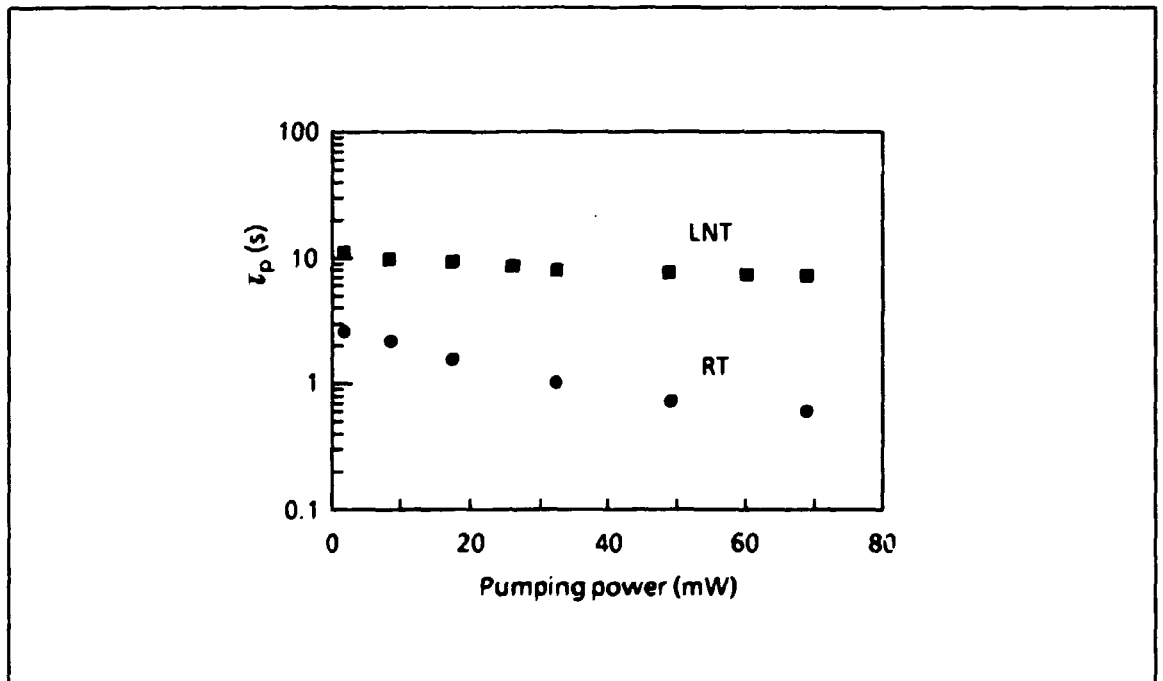


Fig. 14 - Time constant τ_p as a function of pumping power at RT and LNT, obtained from the absorption measurements

pumping power at different temperatures both in the emission and absorption experiments. Figure 13 displays τ_p vs the pumping power at RT and LNT, as taken from luminescence signals. Figure 14 displays τ_p vs pumping intensity at RT and LNT,

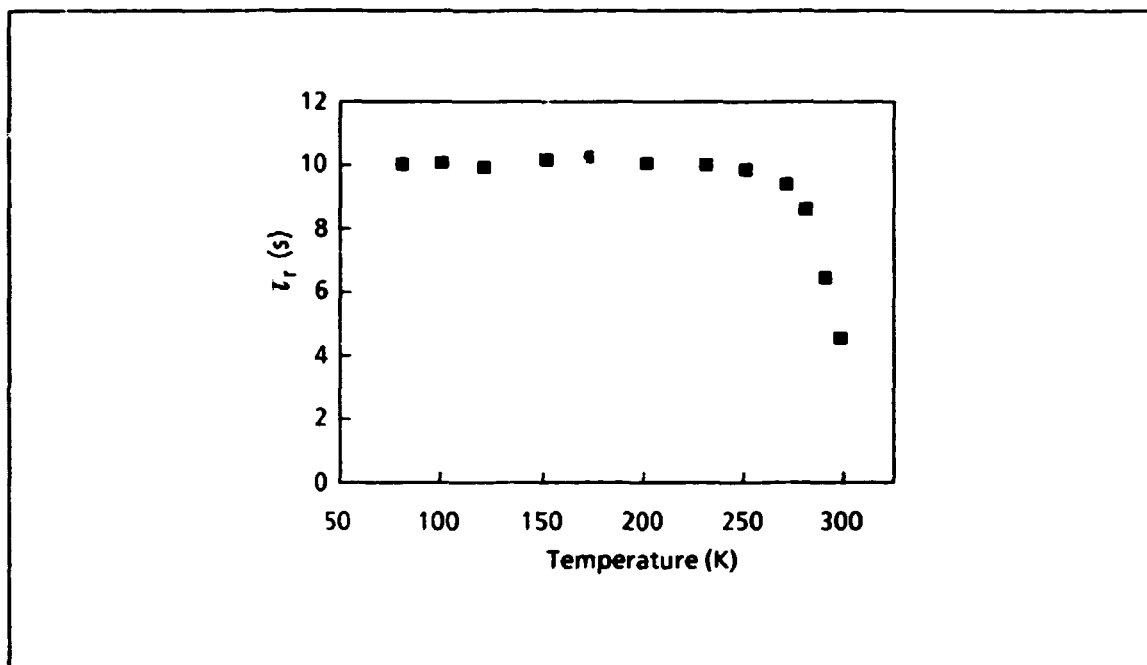


Fig. 15 - Time constant τ_1 , as a function of temperature obtained from the absorption measurements

as taken from absorption signals. As expected, the two set of data are in good agreement especially by taking into account that the experimental conditions are not completely identical in the two cases, and that especially at low pumping powers the experimental errors are quite big.

The time constant τ_1 does not depend on the pumping power and its dependence on the temperature is reported in Fig. 15, as taken from absorption signals. However similar results are also obtained for τ_1 with repetitive short pulses of pumping light, by measuring the emission which at the beginning is proportional to the GS population.

4 - DISCUSSION

The experimental results given in the previous section show very clearly that under optical pumping the population in the known optical cycle of the F_3^+ centers decreases, Figs. 7 and 10, that the intensity and time evolution of emission and absorption is strongly dependent on the pumping intensity, Figs. 9,13 and 14, and that the recovery of the GS population happens with a unique time constant, Fig. 12, which is a function of temperature alone, Fig. 15. All these experimental facts indicate the existence of a long lived state able to trap momentarily the electronic excitation, and that this energy level could be a triplet state as has been previously proposed [7,8,14].

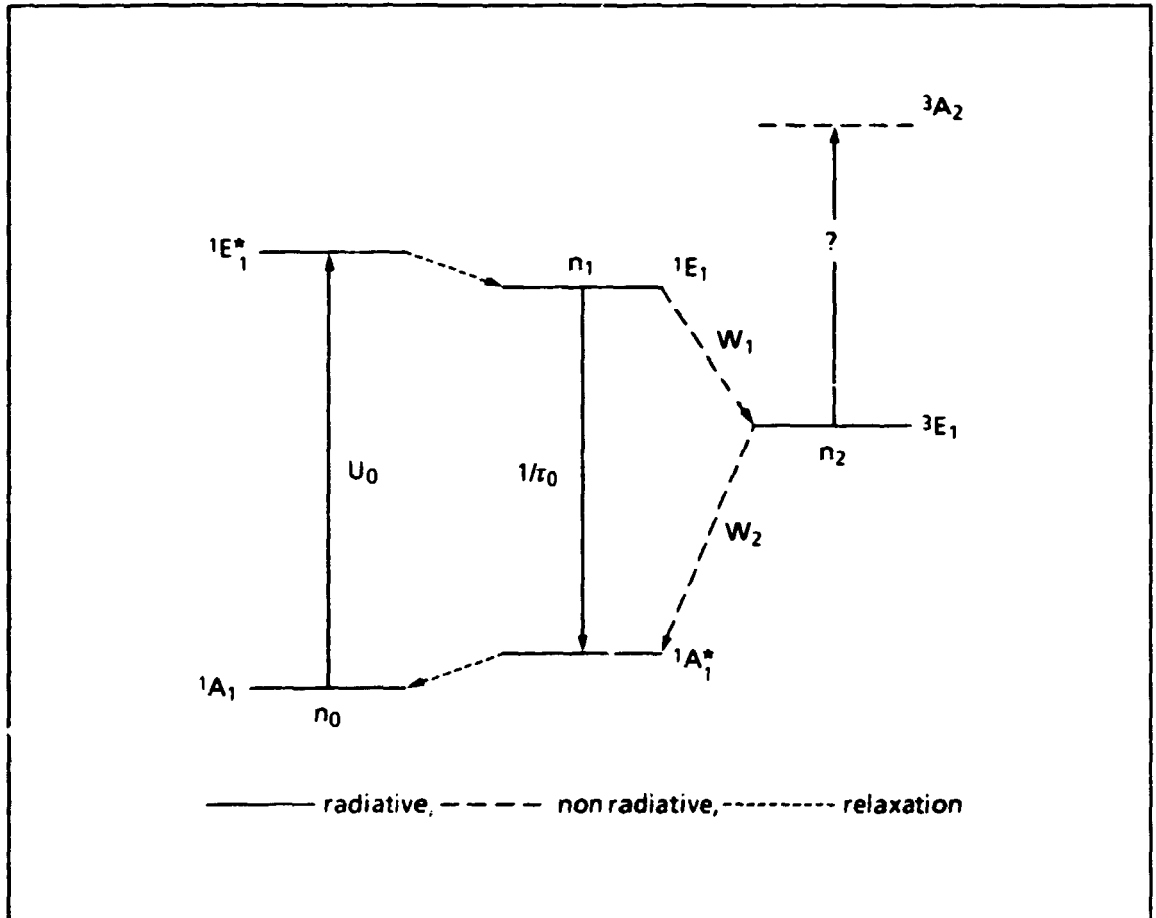


Fig. 16 - Energy levels diagram of the F_3^+ center with illustration of the radiative, nonradiative and relaxation transitions

Figure 16 shows the proposed energy level diagram which contains all the elements necessary for the explanation of the previous results. The F_3^+ center can be excited from the ground state (GS), 1A_1 , to the first excited state, $^1E_1^*$, by optical pumping $U_0 \neq 0$. After a relaxation time of the order of ps, the excitation reaches the relaxed excited state (RES), 1E_1 , from where it can decay radiatively, with the time constant τ_0 of the order of ns, to the unrelaxed ground state (URGS), $^1A_1^*$, or reach through a nonradiative transition, W_1 , the ground triplet state (GTS), 3E_1 . From the triplet state the excitation can reach through another nonradiative transition, W_2 , the unrelaxed ground state, $^1A_1^*$. From here the excitation eventually relaxes to the ground state in a time of the order of ps. So the triplet state acts both as a trap for the excitation population and as an efficient quenching for the emission. The possibility of an optical excitation to the higher energy triplet state, 3A_2 , will not be considered at this stage of the analysis.

By considering that the lifetime τ_0 of the RES is of the order of a few ns, and that the pump rate out of the GS, U_0 , can be at the maximum power used in the present experiments $\sim 10^3 \text{ s}^{-1}$, it follows that only the GS, RES and GTS

states retain an appreciable population during the optical cycle. So by limiting the study only to these three states the rate equations of the optical cycle are:

$$\left\{ \begin{array}{l} \frac{dn_0}{dt} = -U_0 n_0 + \frac{1}{\tau_0} n_1 + W_2 n_2 \\ \frac{dn_1}{dt} = +U_0 n_0 - \left(\frac{1}{\tau_0} + W_1 \right) n_1 \\ \frac{dn_2}{dt} = +W_1 n_1 - W_2 n_2 \\ N = n_0 + n_1 + n_2 \end{array} \right. \quad (1)$$

where the pump rate out of the GS is given by:

$$U_0 = \sigma_0 \cdot \frac{I}{A \cdot h\nu} \quad (2)$$

with $\sigma_0 = 7.1 \cdot 10^{17} \text{ cm}^2$ at $\lambda = 460 \text{ nm}$ [15], and I is the pumping laser power in W , A is the laser focusing area on the crystal, and $h\nu$ the energy of the laser photon. In the present experimental conditions $A = \pi \cdot 10^{-2} \text{ cm}^2$, $h\nu = 4.3 \cdot 10^{-19} \text{ J} (\lambda = 457 \text{ nm})$ so:

$$U_0 = 5260 \cdot I \text{ s}^{-1} \quad (3)$$

Due to the limitation of the present Argon laser output power the maximum value of U_0 is always below 10^3 , and being also $\tau_0 = 4 \text{ ns}$, as measured here by a phase tag technique, it is always $U_0 \tau_0 \ll 1$ so that saturating conditions can be excluded. Moreover, as will be shown later, also $\tau_0^{-1} \gg W_1, W_2$. Within these largely valid approximations, the solutions to a sudden pumping excitation $U_0 \neq 0$ ($t \geq 0$) and initial conditions $n_1(0) = n_2(0) = 0$, $n_0(0) = N$, are given as in the following:

$$\left\{ \begin{array}{l}
 n_0(t) = N \cdot \frac{1}{1 + U_0 \tau_0 \frac{W_1}{W_2}} \cdot \left[1 + U_0 \tau_0 \frac{W_1}{W_2} e^{-\frac{t}{\tau}} \right] \\
 n_1(t) = NU_0 \tau_0 \cdot \left[-e^{-\frac{t}{\tau_0}} + \frac{NU_0 \tau_0 \frac{W_1}{W_2}}{1 + U_0 \tau_0 \frac{W_1}{W_2}} \cdot e^{-\frac{t}{\tau}} + \frac{1}{1 + U_0 \tau_0 \frac{W_1}{W_2}} \right] \\
 n_2(t) = N \frac{U_0 \tau_0 \frac{W_1}{W_2}}{1 + U_0 \tau_0 \frac{W_1}{W_2}} \cdot \left[1 - e^{-\frac{t}{\tau}} \right]
 \end{array} \right. \quad (4)$$

where:

$$\frac{1}{\tau} = (U_0 \cdot \tau_0 \cdot W_1 + W_2) \quad (5)$$

So the populations of the three states are governed by a fast time, τ_0 , and a much slower one, τ , which coincides with the pumping time τ_p introduced in the previous section, and it will be indicated in this way from now on. Moreover, if the pumping intensity is switched off abruptly, the populations of the GS and GTS change exponentially, as is clearly indicated by Eqs. (1), with a time constant W_2^{-1} , which coincides with the recovery time τ_r introduced previously. Hence, as far as the time constants are concerned, we have the following relationships:

$$\frac{1}{\tau_p} = U_0 \cdot \tau_0 \cdot W_1 + W_2$$

$$\frac{1}{\tau_r} = W_2 \quad (6)$$

However from Eqs. (4) it is also possible to calculate the ratio between the initial and final value of both the luminescence, see Fig. 7, and the absorption, see Fig. 10, which are given by the same expression:

$$\frac{n_1^{\max}}{n_1^{(\infty)}} = \frac{n_0(0)}{n_0^{(\infty)}} = 1 + U_0 \cdot \tau_0 \cdot \frac{W_1}{W_2} \quad (7)$$

where n_1^{\max} is the maximum value of the population of the RES just after switching on the pumping laser. In conclusion, if our model of the F_3^+ optical cycle expressed schematically in Fig. 16 is correct, the experimental results should be explained by Eqs. (4), but Eqs. (6) and (7) are more relevant in practice.

Figures 17a and b show $(\tau_p)^{-1}$ as a function of the pumping intensity at RT from the emission measurements of Fig. 13, and at LNT from the absorption measurements of Fig. 14 respectively. A straight line fits very well the experimental points if errors are taken into consideration. Moreover the intercept at $I = 0$ practically coincides, as required by the present model, with the value of $W_2 = (\tau_p)^{-1}$ measured independently, and reported in Fig. 15.

Figures 18a and b show the ratio of the initial and final values of the F_3^+ luminescence and absorption, at LNT and RT respectively as a function of the pumping intensity. As expected from Eq. (7), there is a linear dependence with an unitary intercept for $I=0$.

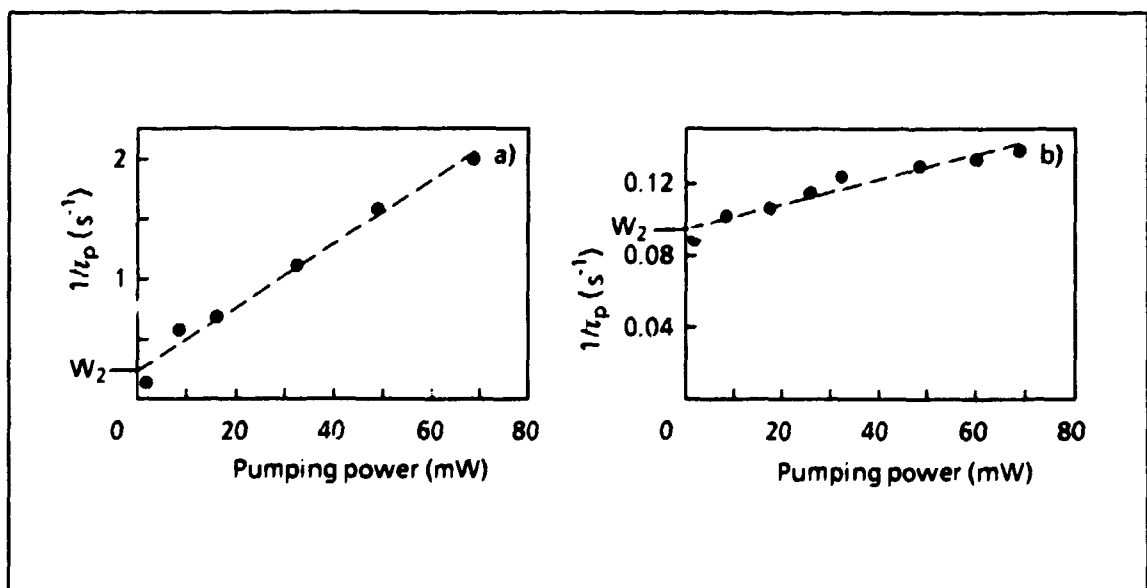


Fig. 17 - Pumping time τ_p as function of laser intensity on the crystal at RT from emission measurements, a, and at LNT from absorption measurements, b. Also the values of $W_2 = (\tau_p)^{-1}$ are shown at $I = 0$.

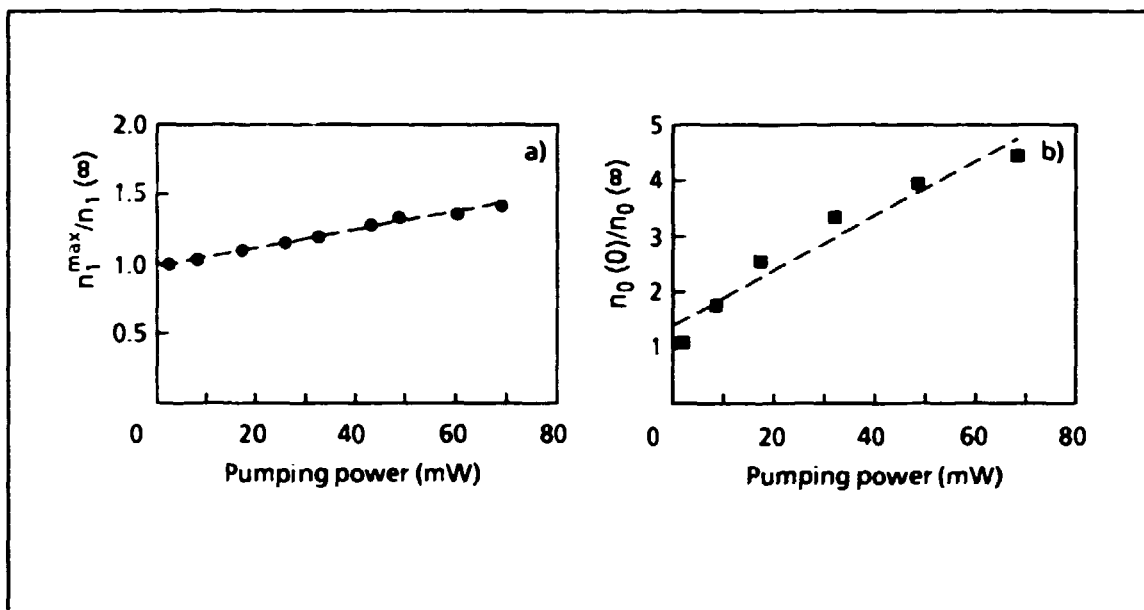


Fig. 18 - Ratio of initial and final intensity of emission, a), and absorption, b), as a function of pump intensity at LNT and RT respectively

Table 1- Numerical values of the transition probability W_1 , obtained from the absorption measurements through Eq. 6, W_1^a , and from the emission measurements through Eq. 7, W_1^e , together with the mean values W_1 and the values of $W_2 = 1/\tau_r$, obtained from absorption measurements, see Fig. 15, at various temperatures

T(K)	W_1^a (10^6 s $^{-1}$)	W_1^e (10^6 s $^{-1}$)	W_1 (10^6 s $^{-1}$)	W_2 (s $^{-1}$)
80	0.46	0.21	0.33	0.10
100	0.60	--	0.61	0.099
120	0.79	--	0.79	0.10
150	1.08	0.85	0.97	0.098
170	1.46	--	1.46	0.097
200	1.89	2.18	2.03	0.099
230	3.24	2.99	3.12	0.10
250	4.18	4.03	4.11	0.10
270	5.28	6.07	5.68	0.11
280	5.82	6.22	6.02	0.11
290	9.70	8.37	9.03	0.15
298	13.56	9.91	11.73	0.22

So the main experimental features of F_3^+ centers are fairly well explained by the present theory, which can be applied to calculate the values of W_1 from the

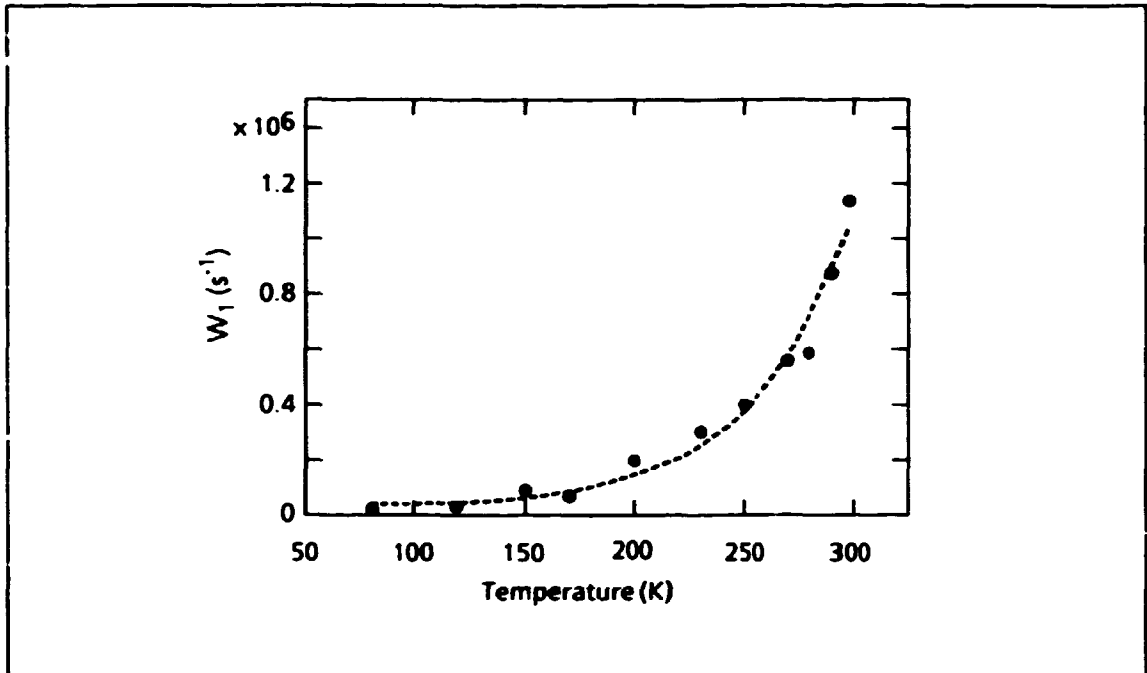


Fig. 19 - Transition probability, W_1 , from the RES towards the GTS as a function of temperature. The dashed line is a fitting of the experimental data with Eq. (8)

measured values $(\tau_p)^{-1}$ and $(\tau_1)^{-1}$ and Eqs. (6) and (7), being the RES lifetime τ_0 a known parameter. The numerical values of W_1 and W_2 are reported in Table 1 at various temperatures. The probability W_1 has been measured both from absorption, Eq. (6), and emission, Eq. (7), measurements and its average value has been also reported, while the probability $W_2=1/\tau_1$ has been obtained from absorption measurements as reported in Fig. 15. Figure 19 reports the average value of W_1 vs temperature, while Fig. 20 shows the values of W_2 in the same graphic representation. It is evident that above 200 K for W_1 and 250 K for W_2 , a multiphonon process is involved in both transitions. The whole behaviour can be explained in the frame of a description which includes a spontaneous process, a one-phonon and a multiphonon assisted process, which can be described by the expression [16,17]:

$$W(T) = W_0 + h_s \cdot \coth\left(\frac{\hbar\omega_s}{2kT}\right) + h_m \cdot \left(1 - e^{-\frac{\hbar\omega_m}{kT}}\right)^{-p} \quad (8)$$

where $\hbar\omega_s$, $\hbar\omega_m$ are the energies of the phonons involved in the one-phonon (single) and multiphonon assisted processes, and p is the number of phonons. A fitting of the experimental data with this formula is reported in Figs. 19 and 20 with dashed lines, and the parameters of the fitting are given in Table 2. It is interesting to note that both the energy, $\hbar\omega$, and the number of phonons involved, p , are different for the two transitions W_1 and W_2 . From these results it is possible, as a first approximation, to

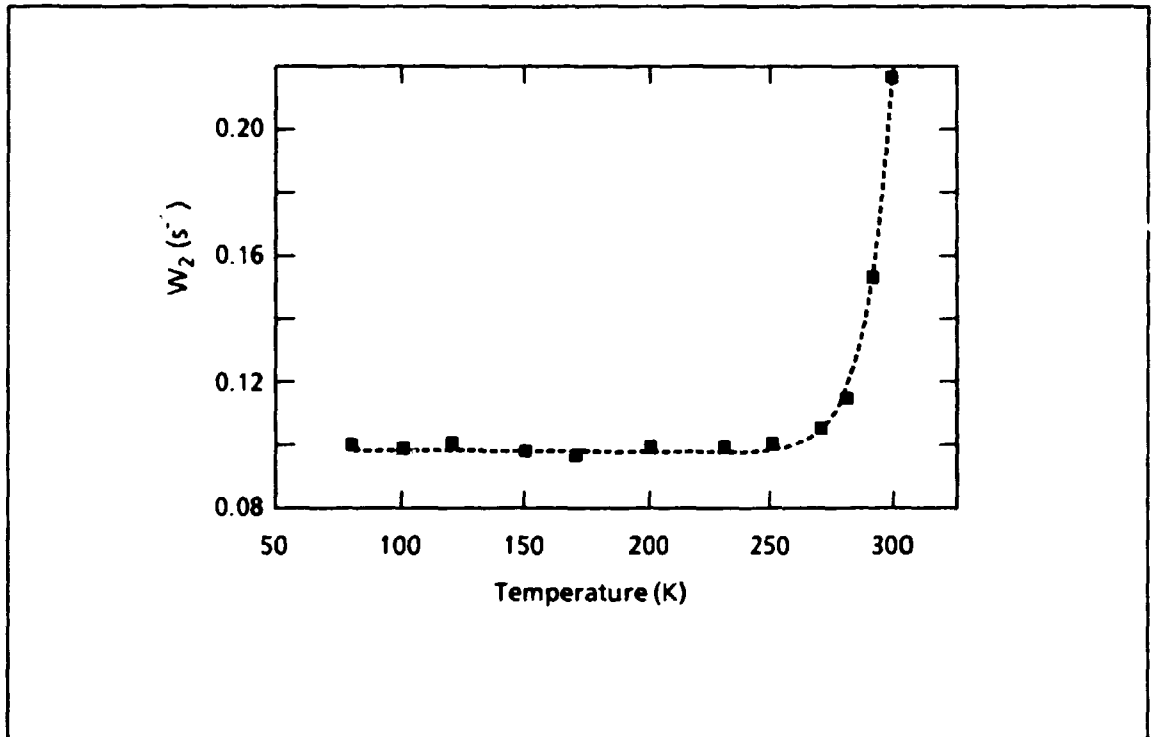


Fig. 20 - Transition probability, W_2 from the GTS towards the URGS as a function of temperature. The dashed line is a fitting of the experimental data with Eq. (8)

Table 2 - Parameters of Eq. (8) derived by fitting the experimental results of Figs. 19 and 20

	$W_1(T)$	$W_2(T)$
W_0 (s^{-1})	0	0.1
h_s (s^{-1})	2	0
$\hbar\omega_s$ [meV]	94.8	-
h_m (s^{-1})	4.2×10^4	2×10^{-10}
$\hbar\omega_m$ [meV]	47.6	28.6
p	19	51

have a measure of the energy separation of the GTS with respect to the RES and the URGS. Indeed $\Delta E_1 = E_{RES} - E_{GTS} \approx p_1 \hbar\omega_{m1} \approx 0.90$ eV, while $\Delta E_2 = E_{GTS} - E_{URGS} \approx p_2 \hbar\omega_{m2} \approx 1.46$ eV, which summed up gives 2.36 eV, almost equal to the emission energy $E_e = 2.34$ eV. The energies of the phonons involved in the two radiationless transitions W_1 and W_2 are $\hbar\omega_{m1} = 47.6$ meV and $\hbar\omega_{m2} = 28.6$ meV, of the same order of magnitude of the phonon modes in LiF, which varies from 24 to 50 meV [18]. This coincidence,

which cannot be completely fortuitous, gives further credit to the formula (8) and to the whole optical cycle of Fig. 16.

5. CONCLUSIONS

Almost all the experimental results of the optical properties of F_3^+ centers in LiF can be explained by introducing a triplet state. More precisely only the ground level of the triplet state seems to play a major role in the optical cycle at the wavelengths and pumping powers used in the present experiments. However we cannot exclude the existence of an excited level for the triplet state, which could explain a time constant of the order of few μs detected in the emission by a phase-tag technique used here, and a small excited state absorption on the short wavelength side of the absorption band [19]. A more complete description of the optical cycle of F_3^+ centers requires further investigations into these details. It is however evident that the ground level of the TS can trap a sizeable fraction of the F_3^+ population and increase, as a consequence, the threshold parameters of the laser emission. Because of the temperature variation of W_1 and W_2 , Figs. 19 and 20, the population of the triplet state decreases while decreasing the temperature. By using Eq. (7) it is possible to calculate the steady state intensity of the emission with respect to its initial value as a function of temperature. The results reported in Fig. 21 for different values of U_0 ,

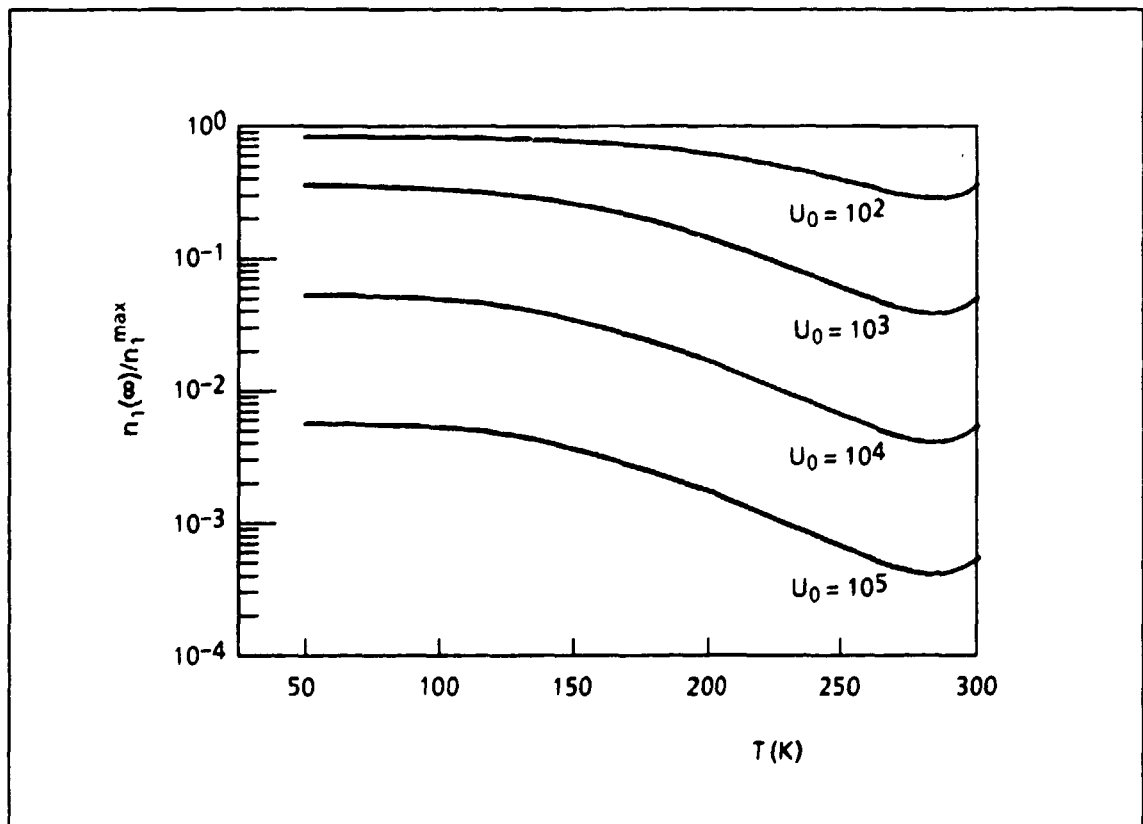


Fig. 21 - $n_1(\infty)/n_1^{\max}$, alias the steady state emission intensity under c.w. laser pumping, as a function of temperature for different values of the pump rate U_0 in s^{-1}

show that the relative intensity of the emission can be one order of magnitude higher at low temperature with respect to RT. These results open the possibility to have a c.w. laser emission at LNT, which is still convenient in LiF crystals, although it poses additional technical problems. By going back to Fig. 21 the small increase of the steady state emission above 270 K is surprising and it deserves to be better investigated experimentally. Indeed such behaviour is justified up to now only by few measurements around RT, so that more precise measurements are needed at and above RT to confirm such unexpected dependence. However it is well known that the possibility of having a bigger emission at temperatures higher than RT is frustrated by the well known instability of the centers at high temperatures under intense optical pumping.

Moreover it should be pointed out that the values of the transition probability W_1 depend among other things on the exact knowledge of the lifetime of the RES, τ_0 , as shown in Eq. (6). Now it turned out through an accurate research of previous works that this parameter is not very well known. Indeed in the first measurement [20], where F_3^+ centers were produced by X rays at RT, $\tau_0=11.5$ ns is independent of temperature from 80 to 200 K. In Ref. 21 and 22 F_3^+ centers in LiF produced by X rays and in presence of Mg and Na impurities give $\tau_0=4\div 10$ ns at RT. In Ref. 3 the value $\tau_0=10$ ns is reported without any sample specification, and in Ref. 23 $\tau_0=4$ ns is measured with a phase tag technique at RT. Moreover recently a sample irradiated with γ rays at 80 K and treated as in section 2 displays, besides the usual F_3^+ band, an absorption at 380 nm which emits at 535 nm with a lifetime of 7.2 ns [24]. This second band has been ascribed to a high lying excited state of the F_3^+ center, so that the observed luminescence is assigned to the RES of the same center. It is clear that there is a dependence on the impurity content in the samples, that the above mentioned measurements were made in crystals not well characterized as far as F_3^+ centers are concerned, and that the present optical cycle was not known until recently. All this means that good lifetime measurements on well prepared samples are required both for basic knowledge and for calculating the crucial transition probability W_1 .

In conclusion, the optical cycle of the F_3^+ centers in LiF is now sufficiently known and, although other measurements are under way to complete its description, the parameters needed for laser action can be derived as a first approximation, so that it is possible to proceed to find out whether a c.w. laser emission is possible or not.

ACKNOWLEDGMENTS

The authors are indebted to Dr. L. Eosi for helpful discussions. Many thanks are due to A. Pace for his technical assistance. One of the author, V. Kalinov is grateful to ENEA for granting him a fellowship

REFERENCES

- [1] L.F. Mollenauer in *Tunable Lasers*, L.F. Mollenauer and J.C. White, eds., Springer Verlag, New York, 1987, p. 225
- [2] A. Arkhangel'skaya and P.P. Feofilov, *Sov. J. Quantum Electron.* **10**, 657 (1980)
- [3] T.T. Basiev, S.B. Mirov, and V.V. Osiko, *IEEE J. Quantum Electron.* **24**, 1052 (1988)
- [4] Yu.L. Gusev, S.I. Marennikov and S.Yu. Novozhilov, *Sov. J. Quantum Electron.* **8**, 960 (1978)
- [5] T. Tsuboi and H.E. Gu, *Appl. Opt.* **33**, 982 (1994)
- [6] G. Baldacchini, in *Advances in Nonradiative Processes in Solids*, B. Di Bartolo, ed., Plenum Press, N.Y., 1991, p. 219
- [7] L.X. Zheng and L.F. Wan, *Opt. Commun.* **55**, 277 (1985)
- [8] S. Paciornick, R.A. Nunes, J.P. von der Weid, L.C. Scavarda do Carmo, and V.S. Kalinov, *J. Phys. D: Applied Phys.* **24**, 1811 (1991)
- [9] J. Nahum and D.A. Weigand, *Phys. Rev.* **154**, 817 (1967)
- [10] A.P. Voitovich, V.S. Kalinov, and I.I. Kalosha, *Soviet Dokl. Akad. Nauk BSSR* **30**, 132 (1986)
- [11] A.P. Voitovich, V.S. Kalinov, S.A. Mikhnov, and S.I. Ovseichuk, *Soviet J. Quantum Electron.* **17**, 780 (1987)
- [12] A. Meyer and R.F. Wood, *Phys. Rev.* **133A**, 1436 (1964)
- [13] J. Nahum, *Phys. Rev.*, **158**, 817 (1967)
- [14] M. Cremona, G. Baldacchini, R.M. Montereali, F. Somma, V. Kalinov, and L.C. Scavarda do Carmo, *Abstracts of the Annual Congress of the National Group of Structure of the Matter*, Monteporzio Catone, Roma, 1991, A41
- [15] H.Yu. Gorkov and V.A. Chepurnoi, *Opt. Spectrosc.* **67**, 642 (1989)
- [16] B. Di Bartolo and R. Peccei, *Phys. Rev.* **6A**, 1770 (1965)
- [17] U.G. Caldino and J.O. Rubio, *Rad. Eff. & Def. Sol.* **127**, 83 (1993).
- [18] *Physic of Color Centers*, W.B. Fowler, ed., Academic Press, N.Y., 1968, p.267
- [19] T.T. Basiev, Private communication (1994)
- [20] L. Bosi, C. Bussolati, and G. Spinolo, *Phys. Lett.* **32A**, 159 (1970)
- [21] T. Kurobori, Y. Imai, and N. Takebuchi, *Opt. Commun.* **64**, 259 (1987)
- [22] T. Kurobori, T. Kanasaki, Y. Imai, and N. Takebuchi, *J. Phys. C: Solid State Phys.* **21**, L397 (1988)
- [23] E. Martins, *Tesi di Mestrado*, Universidade de Sao Paulo, Instituto de Fisica, 1990, p. 85
- [24] A.G. Bazylev, V.S. Kalinov, S.A. Mikhnov, S.I. Ovseichuk, and L.C. Scavarda do Carmo, *J. Appl. Spectr.* **57**, n.5-6, 894 (1992)



Edito dall'Enea, Direzione Relazioni Esterne
Viale Regina Margherita, 125 - Roma
Finito di stampare nel mese di agosto 1995
presso il Laboratorio Tecnografico

L

T 3 4 4

9 5

1 2 0 8